On the Capacity Degradation in Broadband MIMO Satellite Downlinks with Atmospheric Impairments

A. Knopp[1,2)], R.T. Schwarz[1,2)], and B. Lankl[2)]
Email: {andreas.knopp, robert.schwarz, berthold.lankl}@unibw.de

[1)] Federal Office of the German Bundeswehr
for Information Management and Information Technology,
Satellite Communications Division, 56026 Koblenz, Germany.

[2)]Institute for Communications Engineering,
Munich University of the German Bundeswehr,
85579 Neubiberg, Germany.

***Abstract*—We investigate the impact of atmospheric impairments on the theoretical bandwidth efficiency of Multiple-Input Multiple-Output (MIMO) geostationary satellite links which are shaped to optimize the channel bandwidth efficiency. We analyze the impairments caused by precipitation, since this is the most severe atmospheric effect causing capacity degradations. By theory, the MIMO channel capacity is strongly affected by signal attenuation as well as signal phase shifts that might reduce the number and strength of spatial subchannels (eigenmodes). We will show, however, that the characteristics of the phase disturbances prevent a loss of capacity. Regarding the additional attenuation, which the signals may encounter passing through the troposphere, we will quantify outage values for several levels of link capacity degradation. Although a loss of capacity cannot be avoided in total, it still turns out that MIMO systems outperform conventional Single-Input Single-Output (SISO) designs in terms of reliability. Even in the presence of atmospheric perturbations, MIMO systems still provide enormous capacity gains and vast reliability improvements. Thus, the MIMO satellite systems presented are perfectly suited to establish the backbone network of future broadband wireless standards (e.g. DVB-SH), supporting high data rates for a variety of worldwide services.**

I. Introduction

Multiple-Input Multiple-Output (MIMO) radio communications systems have recently attracted high interest due to their potentially higher data rates in comparison with Single-Input Single-Output (SISO) systems. By theory, the channel capacity can be increased linearly with the number of antenna elements used at the transmitter (Tx) and the receiver (Rx) without increasing the transmit power or the allocated frequency bandwidth [1]. Current focus on satellite communication (SatCom) systems recognizes a demand for higher data rates. Especially broadband wireless access, as desired for any services tailored for numerous users, presumes a powerful backbone network capable to bridge long-distance and high-rate data transmission. Future internet services, television broadcast or voice-over-IP are only few examples for possible applications that are tackled in the upcoming DVB-SH standard already nowadays. Hence, it appears to be appropriate to apply the MIMO technology to SatCom systems in order to increase the available data rate and bandwidth efficiency.

It has already been shown in [2] that the construction of MIMO satellite uplinks and downlinks, which are optimal in respect of the maximum achievable MIMO channel capacity, is generally possible for *regenerative* payload designs. The optimization is based on a strong Line-of-Sight (LOS) signal component - the backbone of any SatCom radio link. In [3] this concept has been extended to *transparent* communication payloads, accompanied by a number of application examples. By then it has become apparent that also under conditions of undisturbed LOS propagation the construction of capacity-optimal MIMO SatCom systems is viable, which provides an addition to the well-referenced standard literature on SatCom (e.g. [4]), where the benefits of the MIMO technology have primarily been outlined for the rich-scattering fading channel.

Though, likewise SISO links, also the MIMO channel capacity is supposed to degrade under impairments within the propagation channel. No results have been published yet investigating and quantifying the impact of channel perturbations on capacity-optimal MIMO links. In this paper we present such analyses, particularly addressing links between two satellite antennas in the geostationary orbit and an arbitrary number of ground terminal antennas.

A. Atmospheric Phenomena Investigated

Any electromagnetic wave propagating from the satellite down to earth or vice versa must pass through various atmospheric zones at different altitudes. Within a frequency range of 1GHz to 30GHz only two regions have to be taken into account due to their notable impact on the propagation properties of a radio wave. These are namely the *troposphere* and the *ionosphere* [5]. In the troposphere all kinds of weather effects are present: rain, snow, ice, hail and fog or clouds. Within the ionosphere the radio waves are mainly influenced by the total electron content (TEC), i.e. the number of free electrons. The severity of the influence is strongly dependent upon the radio frequency; higher frequencies are generally advantageous in terms of undisturbed propagation through the ionosphere. On the contrary, for the troposphere the disturbances of the radio waves become more severe as the frequency increases. They cannot be neglected for frequencies above 10GHz [5]. In this paper we consider a typical downlink at a carrier frequency of 14GHz within the Ku frequency band (12GHz. . .18GHz [6]). For those frequencies it is sufficient to concentrate on the tropospheric impairments, in particular the weather conditions, since the attenuating influence of the

978-1-4244-6404-3/10/$26.00 ©2010 IEEE

ionosphere on the radio waves can be neglected [7]. Phase disturbances, however, are very severe in the ionosphere.

B. Signal Attenuation

The weather conditions of the troposphere can basically be categorized roughly into either *clear sky* conditions with low rainfall rates and negligible atmospheric effects on the channel capacity, or *rain* conditions (0.01% of a year) at least characterized by a significantly increased signal attenuation. The most important weather effect violating the propagation properties is signal attenuation caused by precipitation (rain and wet snow), while the other tropospheric effects can usually be neglected [7]. To provide an example, an additional attenuation due to clouds and fog not exceeding 1% of an average year of 0.2dB for 12GHz can be observed at an elevation angle of about 20°. The values for the frequencies of 20GHz and 30GHz are 0.5dB and 1.1dB, respectively [5]. As a first approach covering the most relevant tropospheric influences, therefore, it is reasonable to limit the discussion to precipitation impairments.

C. Signal Phase Disturbances

Apart from additional attenuations in the channel, phase angle disturbances are crucial in MIMO system architectures. According to [2] and [3] any capacity-optimal MIMO link demands a particular structure of the phase angle relations within the MIMO channel transfer matrix in order to provide numerous and powerful spatial subchannels (eigenmodes). If this structure is disturbed by the atmosphere (ionosphere or troposphere), at a first glance the channel capacity is expected to collapse. However, in section IV-B we will show that atmospheric disturbances of the signal phases are innoxious for MIMO satellite systems under practical constraints.

D. Paper Content

Following a brief description of our system model and the MIMO channel capacity calculation in section II, in section III we will introduce an exemplary MIMO downlink scenario that has been optimized in respect of the channel capacity. Section IV comprises an analytical analysis on the capacity under conditions of varying atmospheric attenuation in the different propagations paths of the MIMO satellite channel. Furthermore, the influence of phase disturbances, which the MIMO signals might be subject to when passing through the channel, is analyzed. The results will quantify how MIMO satellite systems outperform SISO systems in capacity, availability and link reliability. Section V concludes the paper.

II. Channel Model and Channel Capacity

All the discussions in this paper are referenced to an exemplary satellite downlink channel without loss of generality. According to [2] and [3] we limit ourselves to $N = 2$ satellite antennas in the geostationary orbit for practical reasons, but allow a theoretically unlimited number M of ground terminal antennas. The results presented in section IV are independent of the kind of satellite system used, signifying their valitity for both *transparent* and *regenerative* payloads.

A. Fundamentals of the MIMO Satellite Channel

Denoting the carrier frequency by f_c, the frequency-flat MIMO channel is described by its channel transfer matrix (CTM) $\boldsymbol{H}(f_c) = \boldsymbol{H} \in \mathbb{C}^{M\times N}$ for a MIMO system consisting of N transmit and M receive antennas. Accounting for the LOS signal part, the element $[\boldsymbol{H}]_{mn}$ of the mn-th matrix entry in equivalent baseband notation is described by the mechanism of free-space propagation according to

$$H_{mn} = a_{mn} \cdot \exp\left\{-j\frac{2\pi f_c}{c_0} r_{mn}\right\} \quad (1)$$

where r_{mn} is the geometrical distance between the n-th Tx antenna and the m-th Rx antenna. c_0 is the speed of light in free-space. a_{mn} is the complex envelope that is calculated by $a_{mn} = c_0/(4\pi f_c r_{mn}) \cdot \mathrm{e}^{j\vartheta_0}$, with ϑ_0 marking the common carrier phase at the time of observation. Because the approximation $r_{mn} \approx r \pm 3\text{km}\ \forall m, n$ is applicable, using $|.|$ to denote the absolute value, it is moreover reasonable to further approximate the channel path gains by

$$|a_{mn}| \approx |a| = \text{const.}\ \forall\ m \in \{1, ..., M\},\ n \in \{1, ..., N\}. \quad (2)$$

B. MIMO Channel Capacity Calculation and Optimization

We basically have to distinguish between MIMO satellite systems utilizing a regenerative payload and systems equipped with transparent payloads [3]. While the transparent payload acts as an amplifying relay, which converts a signal directly from the uplink to the downlink carrier, the regenerative payload demodulates the receive signal to the baseband, decodes and re-modulates it again before transmission down to the receiving ground terminal. Focusing the discussion on the downlink, at this point it is sufficient to investigate the MIMO capacity independently of the particular payload design. The time invariant MIMO spectral efficiency without channel knowledge at the Tx is calculated for a frequency-flat MIMO channel according to Telatar's well-known equation [8]

$$C = \log_2\left[\det\left(\boldsymbol{I}_{M\times M} + \rho \cdot \boldsymbol{H}\boldsymbol{H}^{\mathrm{H}}\right)\right]. \quad (3)$$

$(.)^{\mathrm{H}}$ denotes the conjugate transpose of a matrix and ρ is the linear value of the logarithmic signal-to-noise ratio *SNR*, i.e. $\rho = 10^{(SNR/10)}$. In this paper ρ is defined as the ratio of the transmit power at each transmit antenna and the noise power at each receive antenna. Thus, for the capacity calculations the *SNR* is defined as

$$SNR = EIRP + (G - T) - \mathcal{K} - \mathcal{B} \quad [\text{dB}] \quad (4)$$

where *EIRP* and $(G - T)$ are the dB-values of the effective isotropic radiated power and the figure-of-merit [5], respectively. $\mathcal{K} = 10\log_{10}(\mathfrak{k})$ is the dB-value of Boltzmann's constant $\mathfrak{k}$. Analogously, $\mathcal{B} = 10\log_{10}(B)$ denotes the dB-value of the downlink bandwidth. Hence, the transmit and receive antennas are not counted among the propagation channel; they are part of the transmitter and the receiver. The CTM $\boldsymbol{H}$ is not further normalized because the path loss $\mathcal{L} = 10\log_{10}(|a|^2)$ is incorporated into each channel transfer function $[\boldsymbol{H}]_{mn}$ according to eq. (1). If the capacities of a MIMO and a SISO system are compared, fairness requires to keep the overall transmit power constant for both system types. For that reason, if we calculate the capacity of the SISO system to be compared with a MIMO system, we have to multiply the signal-to-noise-ratio by the number of transmit antennas N used with the MIMO system[1]. Based on this restriction, the channel capacity for a SISO system is calculated

$$C_{\text{SISO}} = \log_2\left(1 + \rho \cdot N \cdot |h_{\text{SISO}}|^2\right) \tag{5}$$

where h_{SISO} is the channel transfer function between the transmit and the receive antenna. Maximum multiplexing gain of the MIMO channel is achieved if all the $\text{rank}(\boldsymbol{Q}) = \min(M, N)$ nonzero eigenvalues $\gamma_i,\ i \in \{1, \ldots, \min(M, N)\}$ of the matrix $\boldsymbol{Q}$ equal $\gamma_i = |a|^2 \cdot \max(M, N)$. In this case we obtain an orthogonal CTM and, thus, it can be deducted that the MIMO channel capacity is maximized by

$$C_{\text{opt}} = \min(M, N) \cdot \log_2\left(1 + \rho\ |a|^2 \max(M, N)\right). \tag{6}$$

For the rest of this paper we will always presume orthogonal (capacity-optimal) MIMO satellite channels. In [2] the practical construction of orthogonal LOS channels based on geometrical deliberations has been thoroughly explained. As a key result this optimization has revealed that large antenna separations are required on earth for the case of multiple antennas onboard a single satellite. A design example is provided in the next section, illustrating the most important presumptions necessary for the analysis of atmospheric impairments.

III. Optimal MIMO Satellite Link: An Example

A. Optimization Procedure

As illustrated in fig. 1, in our scenario the $N = 2$ satellite antennas are mounted on a single satellite. We presume an

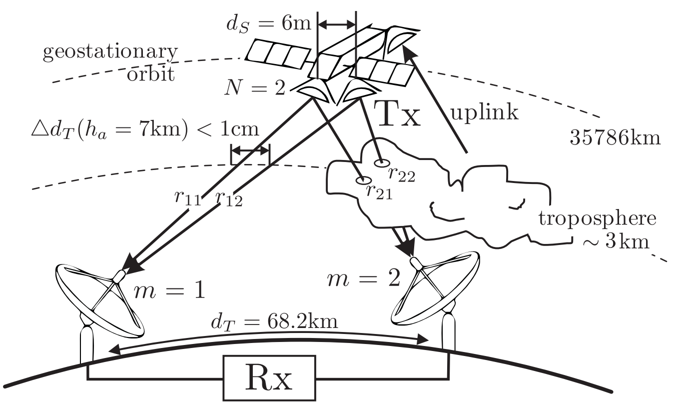

Fig. 1. MIMO scenario with optimal MIMO downlink ($f_c = 14\text{GHz}$)

inter-antenna spacing at satellite side of $d_S = 6\text{m}$ with the satellite beeing located at 13°E and the ground terminal antenna array centered at the geographical position 11.1°E, 47.8°N. Furthermore, the $M = 2$ receiving antennas of the array are lined up in east-west direction. The resulting inter-antenna spacing of the ground terminal antennas is $d_T = 68.2\text{km}$. It has been computed according to the optimization procedure outlined in [2]. For this set of parameters the resulting MIMO downlink channel obtains maximum multiplexing gain leading to C_{opt}. It has to be noted, that the resulting inter-antenna spacing of $d_T = 68.2\text{km}$ on earth in conjunction with the presumed $d_S = 6\text{m}$ spacing at satellite side marks the minimum spacing in order to obtain an orthogonal MIMO CTM. If smaller antenna spacing on earth is desired, the spacing in the geostationary orbit has to be expanded. Of course the scenario could be expanded by further ground terminal antennas, i.e. $M > 2$. Then the resulting antenna spacing d_T on earth becomes smaller according to the relation $d_T^{M\times 2} \cdot 2/M$, for example $d_T^{3\times 2} = 45.5\text{km}$ in case of a 3×2 system and $d_T^{4\times 2} = 34.1\text{km}$ for the 4×2 system. The reader is again referred to [2] and [3] for a deeper discussion.

B. Properties of Atmospheric Impairments

It can be observed for the geometrically optimized downlink scenario provided, that those LOS propagation paths ending at the same Rx antenna are nearly parallel. A simple calculation using the parameter example in fig. 1 demonstrates this fact: Because of $r_{m1} \approx r_{m2} = r_0,\ \forall\ m \in \{1, \ldots, M\}$ the separation $\triangle d_T(h_a)$ of the two rays r_{m1} and r_{m2} at the altitude h_a can be estimated

$$\triangle d_T(h_a) = h_a \cdot \arccos\left(1 - 0.5 \cdot d_S^2/r_0^2\right) \tag{7}$$

with good accuracy, provided that $h_a \ll r_0$. With an antenna separation of $d_S = 6\text{m}$ at satellite side and a realistic altitude of severe weather influences (troposphere) at $h_a = 7\text{km}$, the resulting horizontal separation of the rays r_{m1} and r_{m2} obtains $\triangle d_T(h_a) < 1\text{cm}$. But even at satellite altitude the two rays are separated only $d_S = 6\text{m}$. Therefore, it is very reasonable to assume ***identical atmospheric impairments for all the signals propagating to the same Rx antenna***. This constraint is very crucial for the analyses in section IV.

IV. Analysis of the Capacity in Case of Fading

A. Modeling Approach

Any atmospheric perturbation can basically be modeled as an additional phase shift and an additional channel attenuation acting upon the free-space propagation matrix $\boldsymbol{H}$. For that reason we describe the atmospheric influences on a MIMO channel by means of a matrix $\boldsymbol{X} \in \mathbb{C}^{M\times N}$ consisting of complex-valued entries. The impaired channel matrix $\widetilde{\boldsymbol{H}}$ can then be modeled by an entry-wise multiplication of the free-space channel matrix $\boldsymbol{H}$ and $\boldsymbol{X}$, i.e.

$$\widetilde{\boldsymbol{H}} = \boldsymbol{H} \odot \boldsymbol{X}, \tag{8}$$

applying the Hadamard product operator $\odot$. The matrix $\boldsymbol{X}$ incorporates the atmospheric impact for each of the $M \cdot N$ radio links forming the MIMO channel. Presuming that

[1]A different approach, which is often used, applies ρ instead of $N \cdot \rho$ to the SISO system and consequentially divides ρ by N in the MIMO case (eq. (3)). Likewise in our convention, this way the SISO transmit power is allocated equally to the N MIMO antennas. However, using ρ/N for the MIMO system complicates the formulation of the *SNR* depending on the more sound figure-of-merit of a real link (eq. (4)). In general, the convention used for comparison of the SISO and MIMO cases has no effect on the basic results presented. Thus, we can apply $N \cdot \rho$ as the SISO signal-to-noise ratio.

1. there is no perturbation of the LOS signal paths in the vicinity of the satellite antennas (in the vacuum)
2. the atmospheric influences for all the signals arriving at the same Rx antenna are identical (please refer to section III)

the matrix $\boldsymbol{X}$ can be calculated by:

$$\boldsymbol{X} = \boldsymbol{x}_{\text{Rx}} \cdot (\boldsymbol{x}_{\text{Tx}})^{\text{T}} \quad (9)$$

$$\boldsymbol{x}_{\text{Rx}} = [\alpha_1, \alpha_2, \ldots, \alpha_M]^{\text{T}}, \quad \boldsymbol{x}_{\text{Tx}} = [1, 1, \ldots, 1]^{\text{T}} \quad (10)$$

The vectors $\boldsymbol{x}_{\text{Rx}}$ and $\boldsymbol{x}_{\text{Tx}}$ represent the disturbing influences at the ground terminal and at the satellite side, respectively, i.e. each entry $\alpha_m = |\alpha_m|\mathrm{e}^{-j\phi_m}$ of the vector $\boldsymbol{x}_{\text{Rx}}$ contains the additional path loss $|\alpha_m| \in \{\mathbb{R}_0^+ | 1 \geq |\alpha_m|\}$ and phase shift $\phi_m \in \{\mathbb{R}_0 | -\pi \leq \phi_m < \pi\}$ due to atmospherical impairments at the m-th Rx antenna. In order to calculate the impaired channel capacity $\widetilde{C}$ the matrix $\widetilde{\boldsymbol{H}}$ is inserted into eq. (3):

$$\begin{aligned} \widetilde{C} &= \log_2 \left[\det\left(\boldsymbol{I}_{M\times M} + \rho \cdot \widetilde{\boldsymbol{H}}\widetilde{\boldsymbol{H}}^{\text{H}}\right)\right] && (11)\\ &= \log_2 \left[\det\left(\boldsymbol{I}_{M\times M} + \rho \cdot \boldsymbol{X}_D \boldsymbol{H}\boldsymbol{H}^{\text{H}}\boldsymbol{X}_D^{\text{H}}\right)\right] && (12)\\ &= \log_2 \left[\det\left(\boldsymbol{I}_{M\times M} + \rho \cdot |\boldsymbol{X}_D|^2 \cdot \boldsymbol{H}\boldsymbol{H}^{\text{H}}\right)\right] && (13) \end{aligned}$$

In this case the operator $|\boldsymbol{A}|^2$ is an entry-wise matrix operator denoting the squared absolute value of each entry in the matrix $\boldsymbol{A}$. Furthermore, the matrix $\boldsymbol{X}_D = \operatorname{diag}\{\boldsymbol{x}_{\text{Rx}}\}$ is a diagonal matrix with the elements of $\boldsymbol{x}_{\text{Rx}}$ on the main diagonal. A thorough analysis of the eq. (13) is provided in the next sections, revealing the impact of the atmospheric impairments on the MIMO channel capacity.

B. Impact of Phase Disturbances

In subsection I-C it has been stated that phase angle perturbations might severely degrade the MIMO channel capacity. To further investigate this for the particular case of optimized channels, a very important result can be deducted directly from eq. (13). Letting $|a_m| = 1 \ \forall m \in \{1, \ldots, M\}$, i.e. we assume that there is no additional path attenuation in the channel, the impact of phase shifts comes to the fore. In this case we obtain

$$\boxed{\widetilde{\boldsymbol{H}}\widetilde{\boldsymbol{H}}^{\text{H}} = \boldsymbol{H}\boldsymbol{H}^{\text{H}} \ \Rightarrow \ \widetilde{C} = C} \quad (14)$$

and, thus, by theory ***the MIMO channel capacity is not reduced by atmospheric disturbances of the signal phase***.

C. Impact of Additional Signal Attenuation

Again, we intend to investigate the degradation of the MIMO channel capacity, but this time we assume that the vector $\boldsymbol{x}_{\text{Rx}}$ includes additional path attenuations that are mainly caused by precipitation within the troposphere. As it is directly revealed by the diagonal matrix $|\boldsymbol{X}_D|^2$ in eq. (13), ***the additional path attenuation reduces the signal-to-noise ratio individually at each of the*** M ***receiver inputs***. Only for the case of clear-sky propagation $|\boldsymbol{X}_D|^2 = \boldsymbol{I}$ the maximum MIMO capacity can be obtained. Unfortunately, a simple and practically applicable upper bound expression for the capacity reduction $\triangle\widetilde{C} = C_{\text{opt}} - \widetilde{C}$ as a function of the attenuating vector $\boldsymbol{x}_{\text{Rx}}$ cannot be provided for the very general case of an asymmetric system ($M \neq N$) because $\triangle\widetilde{C}$ cannot be separated easily. However, in case of a symmetric system ($M = N = Z$) a simple closed-form solution can be derived as an approximation[2].

From eq. (9) it is obvious that the matrix $\boldsymbol{X}$ is rank-deficient. We know at the same time that $\boldsymbol{H}$ has full rank, more precisely $\boldsymbol{Q} = \boldsymbol{H}\boldsymbol{H}^{\text{H}}$ has Z nonzero and identical entries only on the main diagonal (remember, we presume an optimal $Z \times Z$ MIMO channel according to section III). If in addition we require the very weak presumption $\boxed{\rho_{\text{Rx}} = |a|^2 \cdot \rho \gg 1}$ and apply a couple of rules of matrix manipulation taken from [9], the channel capacity $\widetilde{C}$ according to eq. (11) can finally be rewritten as

$$\begin{aligned} \widetilde{C} &= \log_2 \left[\det(\boldsymbol{I}_{Z\times Z} + \rho \cdot \widetilde{\boldsymbol{Q}})\right] && (15)\\ &\approx \log_2 \left[\det\left(\rho \cdot \widetilde{\boldsymbol{Q}}\right)\right] = \log_2 \left[\rho^Z \cdot \det(\widetilde{\boldsymbol{Q}})\right] && (16)\\ &= \log_2 \left[\rho^Z \cdot \det(\boldsymbol{Q}) \cdot \left(\prod_{z=1}^{Z} |\alpha_z \mathrm{e}^{-j\phi_Z}|^2\right)\right]. && (17) \end{aligned}$$

Again, Z denotes the number of channel eigenvalues or spatial subchannels available and $\widetilde{\boldsymbol{Q}} = \widetilde{\boldsymbol{H}}\widetilde{\boldsymbol{H}}^{\text{H}}$ is introduced as an abbreviation. Taking eq. (17) as a start, the capacity of the disturbed channel can now be calculated:

$$\widetilde{C} = C_{\text{opt}} - \triangle\widetilde{C}, \quad (18)$$

$$C_{\text{opt}} \approx \log_2 \left[\rho^Z \det(\boldsymbol{Q})\right], \triangle\widetilde{C} = -\sum_{z=1}^{Z} \log_2\left(|\alpha_z|^2\right) \quad (19)$$

$$|\alpha_z| \in \left\{\mathbb{R}_0^+ \mid 1 \geq |\alpha_z| \ \cap \ \triangle\widetilde{C} \ll C_{\text{opt}}\right\}, \quad (20)$$

The optimal channel capacity C_{opt}, given by eq. (6), is reduced by the quantity $\triangle\widetilde{C}$ due to the additional tropospheric path loss. Of course, eq. (18) is only valid as long as $\triangle\widetilde{C}$ stays smaller than C_{opt}. This has to be attributed to the approximation (16). However, in all practical cases with typical additional path attenuations up to 6dB and $SNR_{\text{Rx}} = 10\log_{10}(\rho_{\text{Rx}}) \geq$ 8dB the equations are applicable causing negligible errors.

A very simple upper bound for the capacity degradation $\triangle\widetilde{C}$ as a function of the (maximum) additional attenuation caused by the troposphere and the number of receive antennas faded can be derived as follows: If we denote the number of unfaded receive antennas as L and presume a constant (maximum) additional path gain $|\alpha_0|$ identically for the remaining $M - L$ antennas for simplicity, according to eq. (18) the capacity degradation can be approximated by

$$\triangle\widetilde{C} = -(Z - L) \cdot \log_2\left(|\alpha_0|^2\right), \quad (21)$$

$$|\alpha_0| \in \left\{\mathbb{R}_0^+ \mid 1 \geq |\alpha_0| \ \cap \ \triangle\widetilde{C} \ll C_{\text{opt}}\right\}. \quad (22)$$

In most cases the capacity degradation $\widetilde{C}/C_{\text{opt}} = 1 - \triangle\widetilde{C}/C_{\text{opt}} = 1 - \delta_C$ might be the more relevant figure. δ_C for the case $Z = M = N$ can be approximated by

$$\boxed{\delta_C = \frac{(Z-L)\log_2(10) \cdot \alpha_0^{(\text{dB})}}{10 \cdot C_{\text{opt}}} \approx \frac{(Z-L)\ \alpha_0^{(\text{dB})}}{3 \cdot C_{\text{opt}}}} \quad (23)$$

[2]The case $Z = M = N$ is particularly interesting because it enables a linear increase in channel capacity by the factor Z.

where $\alpha_0^{(\mathrm{dB})} = -20\log_{10}(|\alpha_0|)$ denotes the additional channel path gain in decibel. The right-hand equation provides a very simple, however accurate, method to approximate the percentage of capacity degradation for a symmetric $Z \times Z$ MIMO system which is subject to an additional tropospheric path gain $|a_0|$ at $Z - L$ receive antennas while the remaining L receive antennas are exposed to clear-sky propagation. Fig. 2 shows the relative capacity degradation in % as a

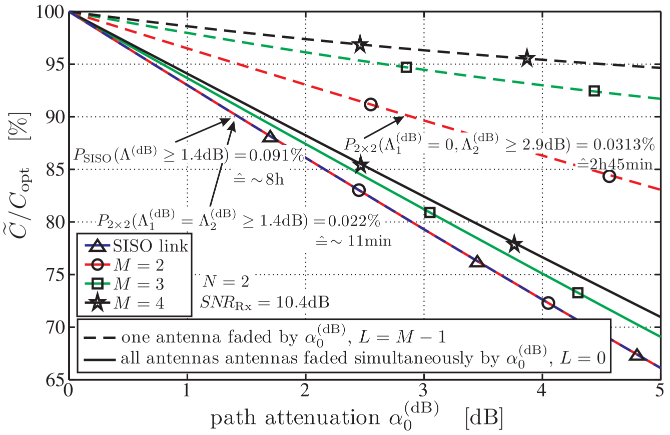

Fig. 2. MIMO capacity degradation due to tropospheric attenuation

function of $\alpha_0^{(\mathrm{dB})}$ simulated also for asymmetric systems with $M > N = 2$. Moreover, different numbers of receive antennas M and fading conditions have been taken into account. It is observed that in case of severe attenuation the MIMO channel capacity quickly degrades, especially if all of the M antennas are attenuated simultaneously. ***However, the degradation is never worse than in the SISO case, which already outlines the superior performance of MIMO systems also in case of fading***. In fact, it is even a worst case scenario to presume that all the M receive antennas are faded by the maximum specific attenuation at the same time, especially for high values of $\alpha_0^{(\mathrm{dB})} > 1\mathrm{dB}$. The probability of simultaneous fades in a MIMO system is substantially lower than for SISO systems. Hence, any statement on the loss in channel capacity is meaningless without accounting for its probability of occurrence. Some of those probabilities are shown in fig. 2, indicating for example that the SISO link and the 2×2 MIMO link actually suffer from the identical relative capacity loss, but the probability of occurrence is more than four times higher in the SISO case. Although it is a very intuitive result that the probability of simultaneous fades decreases with the number and spacing of the antennas, quantifying figures for more than two MIMO antennas are lacking in the literature.

D. Probability of Fades and Link Availability

The goal of the following part is, thus, to calculate the probability or the percentage of time that $M - L$ out of M receive antennas are subject to additional path loss exceeding a particular value. Taking the SISO link as a start, recommendation [10] provides a formula for the calculation of the probability that a specific attenuation caused by rain within an average year at a single location is exceeded. This calculation method is extended to site diversity systems utilizing two ground receivers in [11]. However, there has not been a solution or approximation for the case of more than two receive antennas. Thus, at first we will derive an expression to calculate the probability of simultaneous fades at an arbitrary number M of ground terminal locations using multivariate probability distributions.

The joint probability that the attenuations $\Lambda_m^{(\mathrm{dB})}$ exceeds the values $\alpha_m^{(\mathrm{dB})}$ simultaneously for $m = 1 \dots M$ is given by [11]

$$P(\Lambda_1^{(\mathrm{dB})} \geq \alpha_1^{(\mathrm{dB})}, \dots, \Lambda_M^{(\mathrm{dB})} \geq \alpha_M^{(\mathrm{dB})}) = 100 \cdot P_r \cdot P_a \ [\%], \quad (24)$$

where P_r is the joint probability that it is raining at all M locations and P_a is the conditional joint probability that the attenuations $\Lambda_1^{(\mathrm{dB})}$ to $\Lambda_M^{(\mathrm{dB})}$ exceed the values $\alpha_1^{(\mathrm{dB})}$ to $\alpha_M^{(\mathrm{dB})}$, respectively. Again, the dB-value of each path attenuation is used, i.e. $\alpha_m^{(\mathrm{dB})} = -20\log_{10}(|\alpha_m|)$. We assume that both probabilities P_a and P_r can be modeled by a multivariate normal distribution with the probability density function (pdf)

$$f_{\boldsymbol{Y}}(\boldsymbol{y}) = \frac{1}{(2\pi)^{\frac{M}{2}}\sqrt{\det(\boldsymbol{\Upsilon})}} \exp\left[-\frac{1}{2}(\boldsymbol{y}-\boldsymbol{\mu})^{\mathrm{T}}\boldsymbol{\Upsilon}^{-1}(\boldsymbol{y}-\boldsymbol{\mu})\right] \quad (25)$$

with covariance matrix $\boldsymbol{\Upsilon} \in \mathbb{R}^{M \times M}$ and mean value vector $\boldsymbol{\mu} = [\mu_1 \dots \mu_M]^{\mathrm{T}}$. The probabilities P_r and P_a are the solutions of the complementary multiple integral

$$P_r = \int_{R_1}^{\infty} \dots \int_{R_M}^{\infty} f_{\boldsymbol{Y}}^{(r)}(\boldsymbol{y})\mathrm{d}\boldsymbol{y}, \quad P_a = \int_{A_1}^{\infty} \dots \int_{A_M}^{\infty} f_{\boldsymbol{Y}}^{(a)}(\boldsymbol{y})\mathrm{d}\boldsymbol{y}, \quad (26)$$

where $f_{\boldsymbol{Y}}^{(r)}(\boldsymbol{y})$ and $f_{\boldsymbol{Y}}^{(a)}(\boldsymbol{y})$ with parameter vectors/matrices $\boldsymbol{\mu}^{(r)}, \boldsymbol{\Upsilon}^{(r)}$ and $\boldsymbol{\mu}^{(a)}, \boldsymbol{\Upsilon}^{(a)}$ denote the pdf according to eq. (25) for the rain probability and the probability of attenuation, respectively. Furthermore, the normalized thresholds $R_m = \boldsymbol{\Phi}^{-1}\left[p_m^{\mathrm{rain}}\right]$ and $A_m = \left(\ln(\alpha_m^{(\mathrm{dB})}) - \mu_{\ln\Lambda_m^{(\mathrm{dB})}}\right)/\sigma_{\ln\Lambda_m^{(\mathrm{dB})}}$ are applied. p_m^{rain} is the probability that it is raining at the location of the m-th ground terminal antenna and $\boldsymbol{\Phi}^{-1}$ is the complementary inverse normal distribution. $\ln(\alpha_m^{(\mathrm{dB})})$ is the logarithmic value of the thresholds $\alpha_m^{(\mathrm{dB})}$ with mean $\mu_{\ln\Lambda_m^{(\mathrm{dB})}}$ and standard deviation $\sigma_{\ln\Lambda_m^{(\mathrm{dB})}}$. The values $\mu_{\ln\Lambda_m^{(\mathrm{dB})}}$ and $\sigma_{\ln\Lambda_m^{(\mathrm{dB})}}$ can be determined by fitting each single rain attenuation $\Lambda_m^{(\mathrm{dB})}$ versus probability of occurrence p_m to the log-normal distribution $p_m = p_m^{\mathrm{rain}}\boldsymbol{\Phi}\left[\left(\ln(\Lambda_m^{(\mathrm{dB})}) - \mu_{\ln\Lambda_m^{(\mathrm{dB})}}\right)/\sigma_{\ln\Lambda_m^{(\mathrm{dB})}}\right]$ [11]. A detailed description and a stepwise calculation of $\mu_{\ln\Lambda_m^{(\mathrm{dB})}}$ and $\sigma_{\ln\Lambda_m^{(\mathrm{dB})}}$ are enclosed in [12]. Using these normalized thresholds, $\boldsymbol{\mu}^{(r)}$ and $\boldsymbol{\mu}^{(a)}$ become zero-valued, and the kl-th covariance matrix entries $[\boldsymbol{\Upsilon}^{(r)}]_{kl}$ and $[\boldsymbol{\Upsilon}^{(a)}]_{kl}$ become identical with the respective correlation coefficients [11]

$$\varrho_{kl}^{(r)} = 0.7 \cdot \mathrm{e}^{-\Delta_{kl}/60} + 0.3 \cdot \mathrm{e}^{\lfloor -(\Delta_{kl}/700)^2 \rfloor}, \ \text{and} \quad (27)$$

$$\varrho_{kl}^{(a)} = 0.94 \cdot \mathrm{e}^{-\Delta_{kl}/30} + 0.06 \cdot \mathrm{e}^{\lfloor -(\Delta_{kl}/500)^2 \rfloor}, \quad (28)$$

where $\Delta_{kl} = |(k \cdot d_T - l \cdot d_T)|, \ \ k, l \in \{1 \dots M\}$ and $\lfloor . \rfloor$ is the floor operator. We suggest the study of [10] and particularly [11] for an explanation in-depth on how to compute the probabilities in eq. (24).

As illustrated in fig. 3, we are now able to calculate the probabilities P as a percentage of time of an average year and for a specific attenuation vector $\boldsymbol{\alpha}^{(\mathrm{dB})} = [\alpha_1^{(\mathrm{dB})}, ..., \alpha_M^{(\mathrm{dB})}]^{\mathrm{T}}$ with entries describing the attenuations exceeded at the M locations of the receive antennas simultaneously. We assume

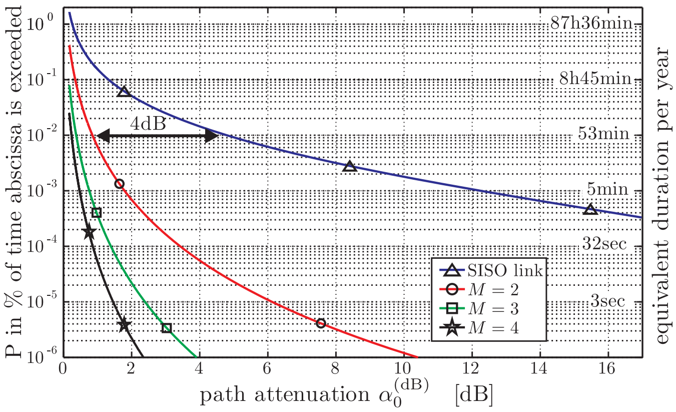

Fig. 3. probability P and equivalent duration per year that a specific additional attenuation $\alpha_0^{(\mathrm{dB})}$ is exceeded simultaneously at all receive antennas, probability of rain $p_m^{\mathrm{rain}} = 0.33,\ \forall m$

a constant mean rain probability of $p_m^{\mathrm{rain}} = 0.33$ for an average year and for all the M locations for simplicity, which is a very high and pessimistic value for the region of 48° latitude. Furthermore, the correlation coefficients in eq. (27) and (28) are calculated using the respective optimum inter-antenna spacing for the appropriate MIMO system example in section III, i.e. $d_T^{2\times 2} = 68.2$km, $d_T^{3\times 2} = 45.5$km and $d_T^{4\times 2} = 34.1$km, respectively. Also a SISO link according to [10] is incorporated in the figure for comparison. Here we have calculated the probability P_a according to [10] and further have multiplied it by the probability of rain presumed ($p_{\mathrm{SISO}}^{\mathrm{rain}} = 0.33$).

The curves show the percentage of time and the equivalent duration per year which a specific attenuation $\alpha_0^{(\mathrm{dB})}$ is exceeded simultaneously for M receiving antennas, where the number of M is varied. The duration of 53min per year corresponds to a 0.01% outage value and marks a specific boundary of relevance for the characterization of SatCom links: If for a target value of $\alpha_0^{(\mathrm{dB})}$ the probability P is smaller than 0.01%, a *high-reliability* system [7] is obtained. Comparing the curve of the SISO link to its MIMO counterparts, outstanding improvements of system reliability become apparent as expected. To provide an example, if a high-reliability link is required, a SISO system would need a 4dB higher margin in the link budget in order to achieve the same robustness as accomplished with a 2×2 MIMO system.

We can conclude that MIMO is appropriate not only to increase the channel capacity but also to enhance remarkably the system reliability and availability. Furthermore, the resulting probabilities qualify the severity of capacity degradations as a function of additional attenuation depicted in fig. 2. Requiring a high-reliability link [7] for a 2×2 MIMO system demands an attenuation margin of 0.7dB. This means that the user has to cope with a capacity falling below $\widetilde{C}/C_{\mathrm{opt}} \cdot 100 = 95\%$ of its optimum value only in less than 53min per year for the presumed *SNR*. In the contrary, a high-reliability SISO link is still very likely to encounter even up to 4.7dB most time of the year in the same situation. This attenuation would then degrade the link performance to an unacceptable extent of approximately 35%. If higher-order MIMO systems are used ($M > 2, N > 2$), these figures further corroborate to the disadvantage of the SISO link.

V. Conclusion

We have analyzed the impact of atmospheric perturbations on the channel capacity of MIMO SatCom systems that in advance have been optimized in respect of their bandwidth efficiency in clear-sky conditions. Although the capacity-focused optimization is mainly based on the construction of appropriate phase angle relations between the multiple transmit and receive signals, any phase disturbances in the ionosphere or troposphere do not degrade the MIMO channel capacity. In the contrary, any additional attenuation that the signals experience in the troposphere might degrade the channel capacity due to a loss in signal-to-noise ratio at the MIMO receiver. However, since large antenna separations at the ground station are required in a single-satellite MIMO system, the capacity gain is accompanied by significant receive diversity effects resulting in very low probabilities of simultaneous fades at all link ends. Thus, MIMO SatCom systems are suited to increase the bandwidth efficiency as well as the link reliability in future long-distance communications systems, granting broadband wireless access for versatile traffic and services.

References

[1] P. Driessen and G. Foschini, “On the capacity formula for multiple input-multiple output wireless channels: a geometric interpretation,” *IEEE Transactions on Communications*, vol. 47, no. 2, pp. 173–176, Feb 1999.

[2] R. T. Schwarz et. al., “Optimum-capacity mimo satellite link for fixed and mobile services,” *International ITG Workshop on Smart Antennas, 2008. WSA 2008.*, pp. 209–216, Feb 2008.

[3] A. Knopp et. al., “Satellite system design examples for maximum mimo spectral efficiency in los channels,” *Global Telecommunications Conference, 2008. IEEE GLOBECOM 2008. IEEE*, pp. 1–6, 30 2008-Dec. 4 2008.

[4] G. E. Corazza, *Digital Satellite Communications*, G. E. Corazza, Ed. Springer, 2007.

[5] G. Maral and M. Bousquet, *Satellite communications systems: systems, techniques and technology*. Wiley, 2002.

[6] ITU-R, “Nomenclature of the Frequency and Wavelength Bands Used in Telecommunications,” International Telecommunication Union, Tech. Rep. ITU-R Recommendation V.431, 2000.

[7] L. Ippolito, “Radio propagation for space communications systems,” *Proceedings of the IEEE*, vol. 69, no. 6, pp. 697–727, June 1981.

[8] I. Telatar, “Capacity of multi-antenna Gaussian channels,” *European transactions on telecommunications*, 1999.

[9] H. Lütkepohl, *Handbook of matrices*. Wiley, 1996.

[10] ITU-R, “Propagation Data and Prediction Methods Required for the Design of Earth-Space Telecomm. Systems,” International Telecommunication Union, Tech. Rep. ITU-R Recommendation P.618, 2007.

[11] ITU-R, “Differential Rain Attenuation,” International Telecommunication Union, Tech. Rep. ITU-R Recommendation P.1815, 2007.

[12] ITU-R, “Probability Distributions Relevant to Radiowave Propagation Modelling,” International Telecommunication Union, Tech. Rep. ITU-R Recommendation P.1057, 2001.